Available online at www.sciencedirect.com
SCIENCE DIRECT®
C. R. Physique 6 (2005) 848–863
COMPTES RENDUS PHYSIQUE
http://france.elsevier.com/direct/COMREN/

Spectroscopy and planetary atmospheres/Spectroscopie et atmosphères planétaires

Atmospheric non-local thermodynamic equilibrium emissions as observed by the Michelson Interferometer for Passive Atmospheric Sounding (MIPAS)

Manuel López-Puertas [a,*], Bernd Funke [a], Sergio Gil-López [a], Miguel Á. López-Valverde [a], Thomas von Clarmann [b], Herbert Fischer [b], Hermann Oelhaf [b], Gabriele Stiller [b], Martin Kaufmann [c], M.E. Koukouli [d], Jean-Marie Flaud [e]

[a] *Instituto de Astrofisica de Andalucía, CSIC, Apdo. 3004, 18080, Granada, Spain*
[b] *Institut für Meteorologie und Klimaforschung, Forschungszentrum Karlsruhe und Universität Karlsruhe, Karlsruhe, Germany*
[c] *Research center Jülich (ICG-I), Jülich, Germany*
[d] *Laboratory of Atmospheric Physics, Aristotle University of Thessaloniki, Thessaloniki, Greece*
[e] *LISA, University Paris 12 & 7 and CNRS, 61, avenue du Général de Gaulle, 94010 Créteil, France*

Available online 6 October 2005

Abstract

In this article we report the most recent advances of our knowledge of non-LTE atmospheric emissions gained from the MIPAS spectra on the Envisat satellite. These include improvements in our knowledge: of the collisional processes between the CO_2 (10^01), (02^21), and (02^01) vibrational levels; of the nascent distribution and collisional relaxation of the O_3 vibrational states; and of the vibrational–vibrational energy transfer rates between $H_2O(020)$ and O_2. In addition we report: the first evidence of mesospheric CH_4 ν_4 7.6-μm emission; much lower non-LTE populations of the $NO_2(v_3 = 1\text{–}4)$ in the daytime stratosphere than previously thought; the first experimental confirmation of the non-LTE excitation of NO(1) in the daytime stratosphere; and the first detection of the CO first hot band non-LTE emission near 4.7 μm. ***To cite this article: M. López-Puertas et al., C. R. Physique 6 (2005).***

© 2005 Académie des sciences. Published by Elsevier SAS. All rights reserved.

Résumé

Observations par le Michelson Interferometer for Passive Atmospheric Sounding (MIPAS) d'émissions atmosphériques par des espèces hors Equilibre Thermodynamique Local. Dans cet article nous présentons les avancées les plus récentes apportées par les spectres fournis par MIPAS sur le satelitte Envisat pour ce qui concerne les émissions de rayonnement par des molécules atmosphériques hors ETL. Il s'agit du progrès de nos connaissances des processus collisionnels entre les niveaux vibrationnels (10^01), (02^21), et (02^01) de CO_2 comme de la distribution initiale et de la relaxation des états vibrationnels de O_3 et des transferts vibration-vibration d'énergie entre $H_2O(020)$ et O_2. De plus, nous présentons : la première mise en évidence de l'émission mésosphérique dans la bande ν_4 de CH_4 vers 7.6-μm ; des populations non-ETL de $NO_2(v_3 = 1\text{–}4)$

* Corresponding author.
E-mail addresses: puertas@iaa.es (M. López-Puertas), bernd@iaa.es (B. Funke), sgl@iaa.es (S. Gil-López), valverde@iaa.es (M.Á. López-Valverde), thomas.clarmann@imk.fzk.de (Th. von Clarmann), Herbert.Fischer@imk.fzk.de (H. Fischer), hermann.oelhaf@imk.fzk.de (H. Oelhaf), gabriele.stiller@imk.fzk.de (G. Stiller), m.kaufmann@fz-juelich.de (M. Kaufmann), mariliza@auth.gr (M.E. Koukouli), flaud@lisa.univ-paris12.fr (J.-M. Flaud).

1631-0705/$ – see front matter © 2005 Académie des sciences. Published by Elsevier SAS. All rights reserved.
doi:10.1016/j.crhy.2005.07.012

observées dans la stratosphère pendant le jour beaucoup plus faibles que ce que l'on attendait ; la première confirmation expérimentale de l'excitation non-ETL du NO(1) stratosphérique pendant le jour ; et la première détection de l'émission non-ETL dans la première bande chaude de CO vers 4.7 µm. ***Pour citer cet article : M. López-Puertas et al., C. R. Physique 6 (2005).***
© 2005 Académie des sciences. Published by Elsevier SAS. All rights reserved.

Keywords: Non-LTE; MIPAS; CO_2; O_3; H_2O; CH_4; NO_2; NO; CO

Mots-clés : Non-ETL ; MIPAS ; CO_2 ; O_3 ; H_2O ; CH_4 ; NO_2 ; NO ; CO

1. Introduction

Assuming we can define a local kinetic temperature defined by the Maxwellian statistics of molecular motion at any atmospheric altitude, we say that an emitting vibrational level is in LTE (local thermodynamic equilibrium) when its population is given by Boltzmann's law at the local kinetic temperature. Its emission is then given by the Planck function at the same temperature. If, on the contrary, its population cannot be described by Boltzmann's law at the local kinetic temperature, we then say that it is in non-LTE, and emits a non-LTE emission. LTE normally occurs when collisions are so frequent that the energy level populations are thermalized at the local kinetic temperature, i.e., at the higher pressures of the lower atmospheric altitudes. However, at higher levels, non-LTE becomes important, particularly when we have important excitation sources as the absorption of solar radiation or chemical reactions. The concept of non-local thermodynamic equilibrium (non-LTE) is usually associated to the infrared emissions emitted by planetary atmospheres. More details about the fundamentals of non-LTE can be found in [1–5].

Non-LTE emissions in the Earth's atmosphere are important for several reasons. Apart from its contribution per se to a better knowledge of the atmosphere, they are essential for calculating the thermal cooling and solar heating rates of the middle and upper atmosphere. Furthermore, the rapid growth of infrared detector technology in recent decades allows us today to sound the middle and upper atmosphere using the limb emission measured by infrared sensors on satellites [7,9]. The inversion of these data in terms of temperature and composition profiles depends on non-LTE radiative transfer theory.

Non-LTE processes in the atmosphere were reviewed a few years ago by López-Puertas and Taylor [2]. However, in the last few years, a wealth of infrared atmospheric emissions measurements have been acquired by the MIPAS (Michelson Interferometer for Passive Atmospheric Sounding) instrument [6–8].

MIPAS is a high resolution limb sounder on board the ENVISAT satellite, successfully launched on 1 March 2002 [7,6]. It has several advantages which makes it a very good instrument for studying the atmospheric non-LTE emissions:

(i) its wide spectral coverage (4.15–14.6 µm or 680–2275 cm^{-1}), allowing for measuring emissions from a given compound in different spectral regions;
(ii) high spectral resolution (0.035 cm^{-1}), enabling the discrimination of emissions from different species, and between different bands of the same species; and
(iii) its high sensitivity allowing measurement of emissions in the upper atmosphere where non-LTE emissions are most important (see Table 1).

In addition, MIPAS has a global pole-to-pole spatial coverage and a day and night temporal coverage. MIPAS scans the limb operationally from 6 km up to 68 km and up to 170 km in the upper atmosphere modes of observation. In this article we present a review of the most important advances in atmospheric non-LTE processes that we have learned so far from MIPAS measurements.

Table 1
MIPAS spectral bands

Band	Spectral range (cm^{-1})	NESR [$nW/(cm^2\ sr\ cm^{-1})$]	Major atmospheric emitters/absorbers
A	685–970	50	CO_2, O_3, CFC11, CFC12, CFC22, HNO_3, $ClONO_2$, HNO_4, C_2H_2, C_2H_6, CCl_4, OCS, SF_6, aerosols
AB	1020–1170	24	O_3, N_2O, CFC12, aerosols
B	1215–1500	12	N_2O, H_2O, CH_4, HNO_3, N_2O_5, $ClONO_2$, CF_4, COF_2, HCN
C	1570–1750	4	H_2O, NO_2, O_3, HNO_3, NO
D	1820–2410	4	CO_2, CO, NO, O_3, N_2O, OH, NO^+, H_2O, OCS, COF_2

2. CO_2 4.3-μm emission

Carbon dioxide has many of vibrational transitions in the 4.3 μm spectral region, including its strongest atmospheric bands. It is known (see, e.g., [2]) that these bands start departing from LTE around the stratopause, the departure being particularly important during daytime, when they are pumped by absorption of solar radiation mainly at 4.3 and 2.7 μm. The study of non-LTE processes in these bands is very important because they are usually used for retrieving the CO_2 abundance in the mesosphere and lower thermosphere [10–14]; and also because they affect the populations of CO_2 levels emitting in the 15-μm first and second hot bands, which are used for retrieving the kinetic temperature. Several studies have been conducted for understanding the non-LTE population of the levels emitting at 4.3 μm using measurements taken by wide-band radiometers and spectrometers with moderate spectral resolution (see, e.g., using SAMS and ISAMS data [10–12], SPIRE data [4], and CRISTA data [13]). It is also known that there are many bands contributing to the Earth limb radiance at 4.3 μm but the lack of measurements with good spectral resolution has prevented one from knowing accurately their individual contributions to the Earth limb emission.

The advantage of having a high resolution instrument, like MIPAS, is that emission from all 4.3 μm bands can be measured, so it is the ideal experiment to study the individual populations of these levels. Although still preliminary, with MIPAS we have been able to test the non-LTE models for many CO_2 states giving rise to the emission at 4.3 and 10 μm; and to improve our knowledge of the vibrational–vibrational processes involving CO_2 ν_2 and ν_3 quanta.

We have conducted a study for analyzing the MIPAS spectra in the 4.3-μm region. Non-LTE limb emission spectra at MIPAS resolution were computed and compared with the measurements. The limb radiance calculations were carried out with the KOPRA code [15] and including the appropriate non-LTE populations of the emitting levels computed with the GRANADA non-LTE generic model [16].

Fig. 1 shows a typical daytime spectrum in the 4.3-μm region taken at a tangent height of ∼70 km on 2nd July 2002 at geolocation 47.5°N, 48.7°E and solar zenith angle (SZA) of 32.8°. The emission in the region from ∼2250 to ∼2290 cm^{-1} is mainly due to the fundamental 4.3-μm band of the 636 (second most important) CO_2 isotope. The larger radiance in the center

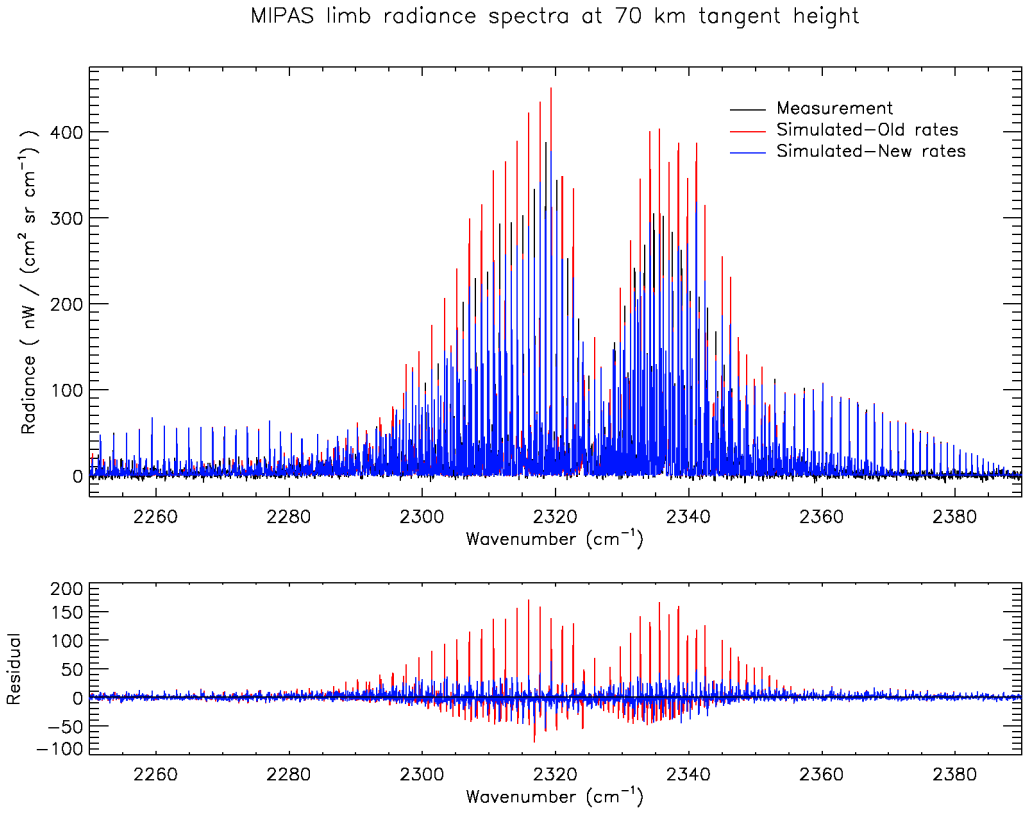

Fig. 1. MIPAS daytime spectra in the 4.3-μm spectral region, dominated by CO_2 bands, at a tangent height of 70 km. Upper panel shows measured (dark grey/black), simulated with old k_1 and k_2 collisional rates (mid-grey/red), and simulated with new collisional rates (light grey/blue) radiance (see text for details). Lower panel: Residual (simulated–measured) radiances. (For interpretation of the references to color, the reader is referred to the web version of this article.)

of the figure is mainly due to the contribution of the major 626 isotope second hot bands: SH1: $02^01 \rightarrow 02^00$; SH2: $02^21 \rightarrow 02^20$; and SH3: $10^01 \rightarrow 10^00$, to the first hot band: FH: $01^11 \rightarrow 01^10$, and to the P-branch of the fundamental band of the major isotope (FB). The minor isotopic fundamental bands (628 and 627) also contribute but to a smaller amount. At wavenumbers larger than ~2350 cm^{-1}, the R-branch of the major isotope fundamental band is the dominant contributor.

In Fig. 1 we also show simulated limb spectra with non-LTE populations computed with the so far accepted collisional relaxation rates for the CO_2 levels responsible for these emissions. In particular, the collisional rates between the upper states of the levels emitting the 4.3-μm second hot bands: 02^00, 02^20, and 10^01:

$$k_1: \quad CO_2(02^01, 10^01) + M \leftrightarrow CO_2(02^21) + M \tag{1}$$

$$k_2: \quad CO_2(02^01) + M \leftrightarrow CO_2(10^01) + M \tag{2}$$

given by 1.5×10^{-13} and 3×10^{-11} $cm^3\,s^{-1}$, respectively. All other non-LTE parameters were taken from the CO_2 non-LTE model as described in [2]. These spectra were calculated using the pressure and kinetic temperature previously retrieved from MIPAS measurements in the 15-μm region as described in [17] and fitting also simultaneously the CO_2 volume mixing ratio (vmr). The concentration of $O(^1D)$, which is known to significantly enhance the population of $CO_2(00^01)$, was calculated by using a photochemical model and the O_3 abundance retrieved from MIPAS spectra in the 10-μm region [18]. Fig. 1 shows that the emission in the region of the SH1 and SH3 second hot bands is, overall, significantly overestimated, although the emission lines in the SH2 second hot band are underestimated. Calculations performed by varying the collisional parameters k_1 and k_2 have shown that a much better fit of the measured spectrum is obtained if using values of 5.5×10^{-13} and 8×10^{-13} $cm^3\,s^{-1}$ for these rates, respectively. These values are very different from previous rates, they differ by factors of 3.5 and 0.025, and represents a significant improvement of the values used before.

When using the new rates, it is remarkable how good the non-LTE model is able to reproduce the Earth daytime 4.3-μm limb spectrum for all bands (see Fig. 2). In this small spectral window, all of the eight lines, arising from seven different bands, the upper states of which are all in non-LTE with different populations, are very well fitted. This clearly shows the enormous usefulness of MIPAS spectra for improving our understanding of non-LTE processes in the atmosphere.

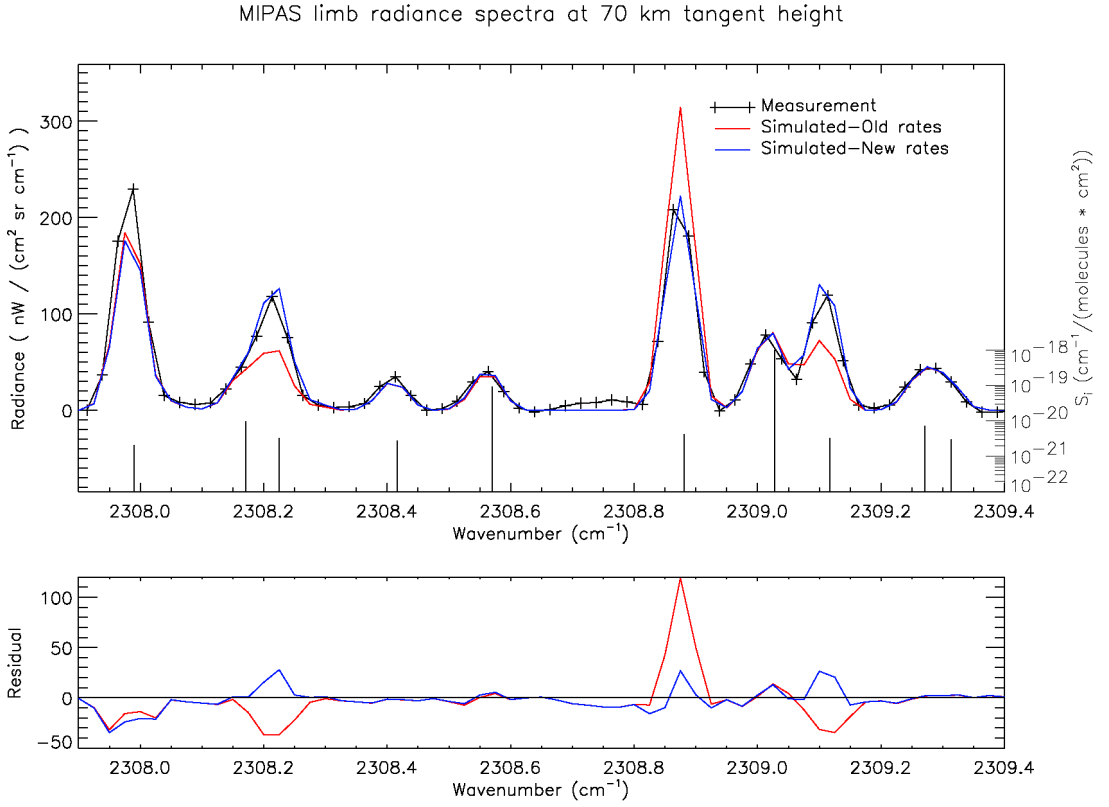

Fig. 2. A zoom of the MIPAS daytime spectra in Fig. 1. The eight emission features in the spectra are due, from left to right, to lines in the following 4.3-μm bands: SH3, SH2, 628, FH, SH1, FB, SH2, and 636, respectively. See text for the meaning of these labels.

3. O_3 5-μm emission

Ozone emission in the 10-μm region is commonly used for measuring its atmospheric abundance (see, e.g., [9,18,19]). Its emission in this spectral region arises mainly from the fundamental band but there are also many hot bands which, due to the non-LTE enhancements of high O_3 vibrational levels after the ozone reaction formation, $O_2 + O + M \rightarrow O_3(v_1, v_2, v_3) + M$, also contribute with a significant amount of radiation. The detailed populations of these levels are not well known, where the nascent distribution and their subsequent collisional relaxation are the two major unknown parameters (see, e.g., [19,2]). The high spectral resolution of MIPAS enables one to discriminate the 001 → 000 emission from the hot bands contribution in the 10-μm region, and is used to derive the O_3 abundance from the stratosphere to the mesosphere [18]. Although MIPAS does not cover the region from 970 to 1170 cm^{-1}, where many O_3 ν_3 hot bands emit, it does cover the 5-μm region (see Table 1), where emission originates from high vibrationally excited O_3 levels. This radiance, together with simultaneous pressure and temperature retrievals and the O_3 abundance derived from the 10-μm 001 → 000 emission, provides an exceptional information to improve our knowledge of O_3 non-LTE processes. Fig. 3 shows averaged spectra in the 2020–2032 cm^{-1} region for day and nighttime conditions taken by MIPAS on 2 July 2003 at a tangent height of ∼56 km. Many highly excited O_3 hot bands contribute to this region as: 002 → 000, 112 → 011, 102 → 001 and 202 → 101. Despite O_3 concentration is larger at nighttime than at daytime at these altitudes, we see a considerable daytime enhancement, which is attributed to the enhanced non-LTE population of the O_3 high energy vibrational levels.

Analogously, Fig. 4 shows similar day and nighttime spectra but in a different spectral region 2120–2126 cm^{-1}. With the exception of the largest radiance of the CO line near 2123.7 cm^{-1}, the daytime enhancement observed at other wavenumbers arises mainly from ro-vibrational transitions of the O_3 101 → 000 band. Hence, these spectra give us information about the populations of the 102 and 101 levels, i.e., from levels close to $v_3 = 3$ and 2, respectively.

A preliminary analysis of O_3 non-LTE processes based mainly in the region of 2080–2130 cm^{-1} (Fig. 4) has been recently carried out by Kaufmann et al. [20]. It has been found that using a typical O_3 non-LTE model, whereby the $O_2 + O$ recombination reaction produces O_3 at $v_3 = 5$ and using the most recent collisional relaxation rates for $O_3(v_1, v_2, v_3)$ [21,22], the MIPAS daytime radiance in this spectral region is underestimated by a factor of 2–3 in the 60–70 km region. Two possibilities have

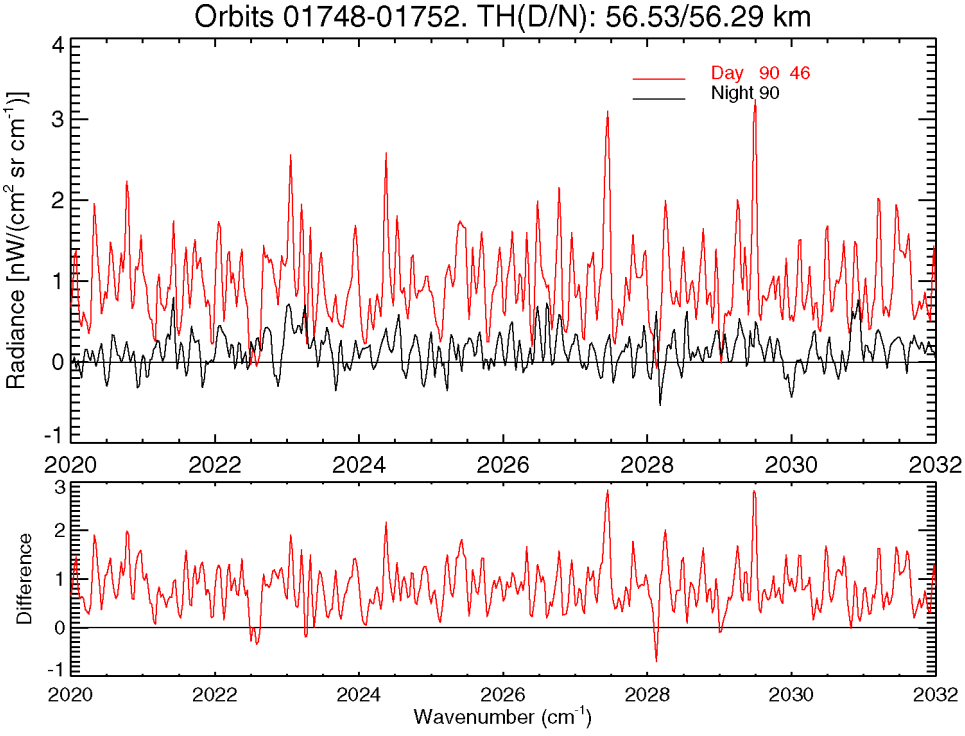

Fig. 3. MIPAS spectra in the 4.9-μm spectral region dominated by the O_3 transitions: 002 → 000, 112 → 011, 102 → 001 and 202 → 101. Upper panel: day (broader trace/red), mean SZA = 46°, and nighttime (fine trace/black) spectrum. 90 spectra were averaged for each case of day and nighttime. Lower panel: day–night difference spectra. The spectra were measured on 2nd July 2002 and cover latitudes from 65°S to 65°N. (For interpretation of the references to color, the reader is referred to the web version of this article.)

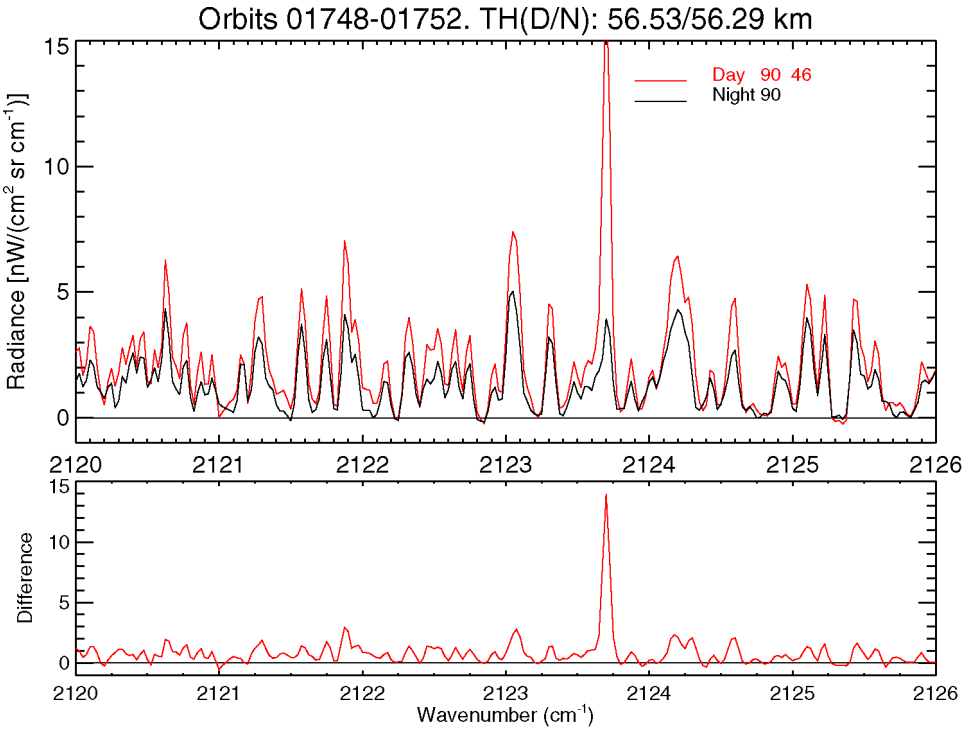

Fig. 4. As Fig. 3 but for the 4.7-μm spectral region dominated by O_3 101 → 000 transitions. The largest peak is a CO transition.

been proposed for increasing the modeled radiances: (i) The O_3 excitation produced after recombination occurs at lower energy levels, e.g., $v_3 = 3$ instead of $v_3 = 5$; or (ii) the stretching (v_1, v_3) to bending (v_2) collisional rates for high vibrational levels have to be reduced by a factor of 3–4. This analysis is still in progress and is being extended to the lower wavenumber region where higher O_3 vibrational levels emit (see Fig. 3). In addition to the relevance of this 5-μm study for improving the accuracy of the O_3 retrieval, it also gives an excellent opportunity to complement laboratory experiments about the O_3 excitation and relaxation mechanisms since these are very difficult to carry out and interpret.

4. H_2O 6.3-μm emissions

The emission of water vapor in the 6.3-μm region is commonly used for retrieving its atmospheric abundance (see, e.g., [7,9]). Water vapor emits in this spectral region mainly from the fundamental (010 → 000) and from the first hot (020 → 010) bands. These emissions have been studied in the past using ISAMS, CIRRIS and CRISTA measurements [23–25], and are known to be in non-LTE at altitudes above around 50–60 km during daytime. However, the large spectral resolution and high sensitivity of MIPAS permits an improvement of our knowledge of non-LTE processes in the H_2O 6.3-μm emissions to be achieved. Fig. 5 shows a mean of 90 spectra for day and nighttime at an approximate altitude of 66 km in the 1600–1630 cm^{-1} spectral region (upper panel). One can easily distinguish the contributions of the different lines in the fundamental and first hot transitions. Although it has been shown in previous measurements and studies that both transitions contribute to the Earth's radiance, it has never before been shown so neatly. The day–night difference spectrum (lower panel) is dominated by the first hot lines. Their emission at nighttime is negligibly small while at daytime they emit a significant radiance because of the absorption of solar radiation at 2.7 μm that excites $H_2O(001)$, and then relaxes via collisional processes to $H_2O(020)$.

The day–night difference in the integrated radiance, after summing over all first hot band lines in the MIPAS spectral range, is shown in Fig. 6 as a function of latitude. It can be noted that the daytime enhancement occurs at altitudes above ∼45 km, reaching values close to 250% of the mean day/night radiance in the upper mesosphere. The lower radiance (−40%) in the lower stratosphere at northern mid-latitudes during daytime are due to a colder daytime kinetic temperature in this region (see also, Fig. 9). A detailed analysis of these measurements has been recently carried out by Koukouli et al. [26] in order to improve our knowledge of the non-LTE excitation of the (020) level. This state is mainly affected by the rate of the vibrational–vibrational collisional process:

$$k'_{vv}: \quad H_2O(020) + O_2 \leftrightarrow H_2O(010) + O_2(1) \tag{3}$$

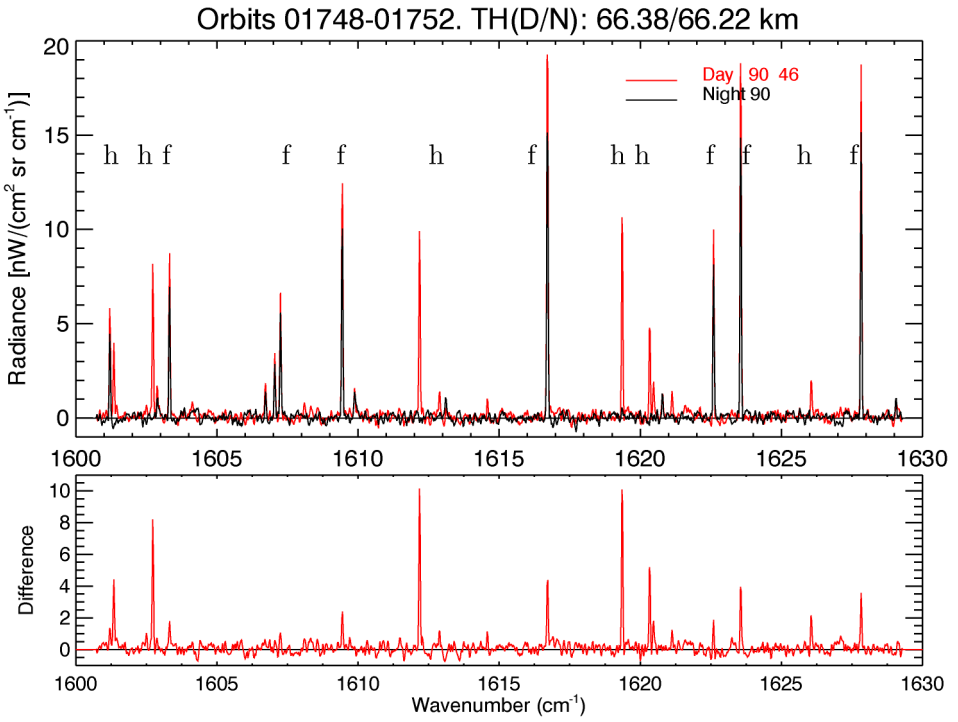

Fig. 5. MIPAS spectra in the 6.2-μm region dominated by H_2O fundamental (010 → 000) (f) and first hot (020 → 010) (h) transitions. Upper panel: 90 measurements were averaged for each case of daytime (dotted/red lines) and nighttime (solid/black lines) to compile the mean spectra. Lower panel: day–night difference spectrum. The spectra were measured on July 2nd 2002 and cover latitudes from 65°S to 65°N. The mean solar zenith angle is 46°. (For interpretation of the references to color, the reader is referred to the web version of this article.)

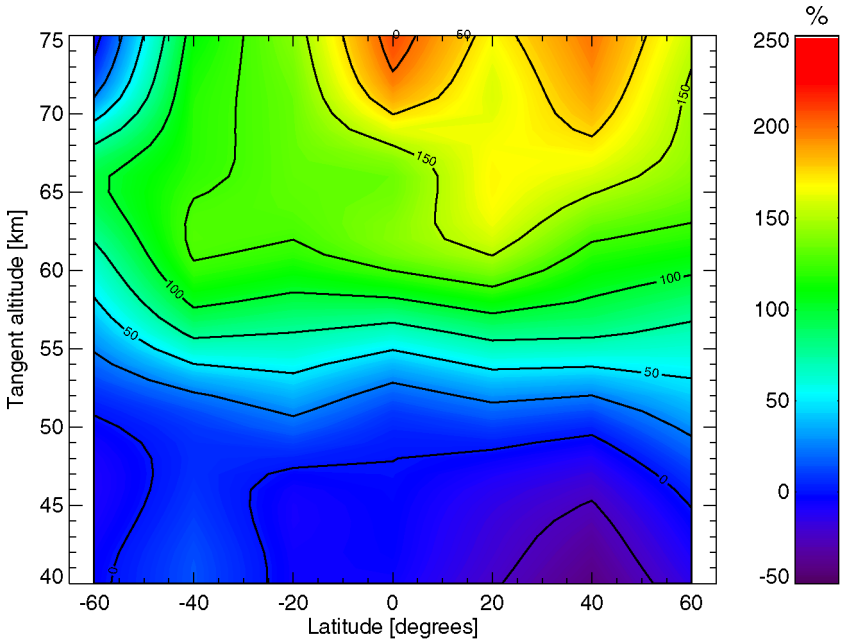

Fig. 6. Zonal mean day–night radiance differences as a function of latitude and tangent altitude in the H_2O (020 → 010) first hot band centred around 6.3 μm in % of the mean daytime/nighttime values. The measurements are from 2 July 2002.

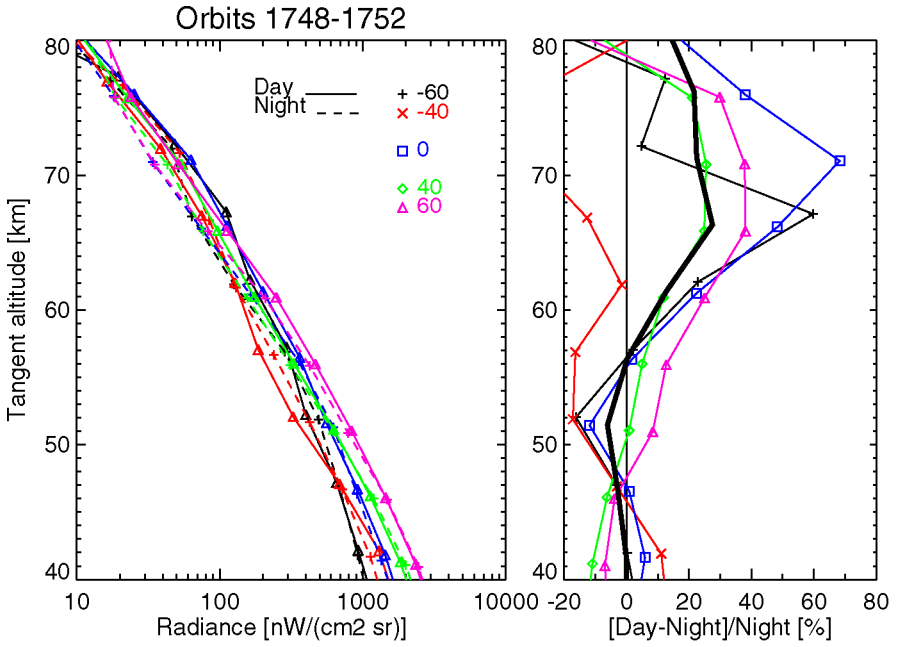

Fig. 7. Spectrally integrated day- and nighttime radiance profiles for the H_2O (010 → 000) fundamental band at selected latitude bands shown in the legend of the left panel. The daytime (solid lines) enhancement as a percentage of nighttime (dashed lines) values is shown in the right panel, with the thick line depicting the average over all latitude bands. The measurements are from 2 July 2002.

The optimal quality (high spectral resolution and large signal/noise ratio) of the MIPAS upper atmosphere measurements have permitted the determination of this rate with a value of 1.36×10 cm^3 s^{-1} and an uncertainty of only 10% [26]. Values determined from previous experiments range between 1 and 3×10^{-12} cm^3 s^{-1}.

The lines of the fundamental band also show a significant daytime enhancement albeit a smaller one (Fig. 5). This is more clearly seen when integrating the radiance over all of the transitions in the band recorded within the MIPAS spectral range (Fig. 7). This figure demonstrates clearly that the fundamental band daytime enhancement is significant above ∼55 km and increases up to ∼40–50% in the upper atmosphere. Understanding this enhancement is very important in order to retrieve accurate daytime mesospheric water vapour abundances from its 6.3-μm emission. There are several processes contributing to this enhancement. The population of $H_2O(010)$ is enhanced by absorption of solar radiation at 6.3 μm, and at 2.7 μm following the collisional relaxation of process (3). It is also enhanced after the photo-dissociation of O_3 and subsequent transfer of energy from the photolysis products to $O_2(1)$ and from this to $H_2O(010)$ by:

$$k_{vv}: \quad H_2O(010) + O_2 \leftrightarrow H_2O + O_2(1) \tag{4}$$

In turn $O_2(1)$, radiatively inactive, is controlled by thermal collisions, mainly with atomic oxygen:

$$k_{vt}: \quad O_2(1) + O \leftrightarrow O_2 + O \tag{5}$$

An analysis of this non-LTE enhancement in the H_2O fundamental band has also been carried out by Koukouli et al. [26]. This work has demonstrated that the observed non-LTE enhancements can be explained using the rate recently measured by Pejaković et al. [27] for process (5), a mean value of 5 $O_2(1)$ molecules produced after each O_3 photodissociated molecule (note that the internal energy available in the photo-dissociation products can excite up to 10 $O_2(1)$ molecules), and the rate of the vibrational–vibrational energy transfer (process (4)), $k_{vv} = k'_{vv}/2$, with k'_{vv} derived from MIPAS measurements of the first hot H_2O emissions [26].

5. CH_4 7.6-μm emission

CH_4 has been measured in the stratosphere using its infrared emissions from the ν_4 band but very scarcely in the mesosphere [28,29]. In consequence, non-LTE processes in this band have been studied very little. Recent theoretical models have predicted that this band departs from LTE in the lower mesosphere and above [30,31]. These predictions had not been confirmed, however,

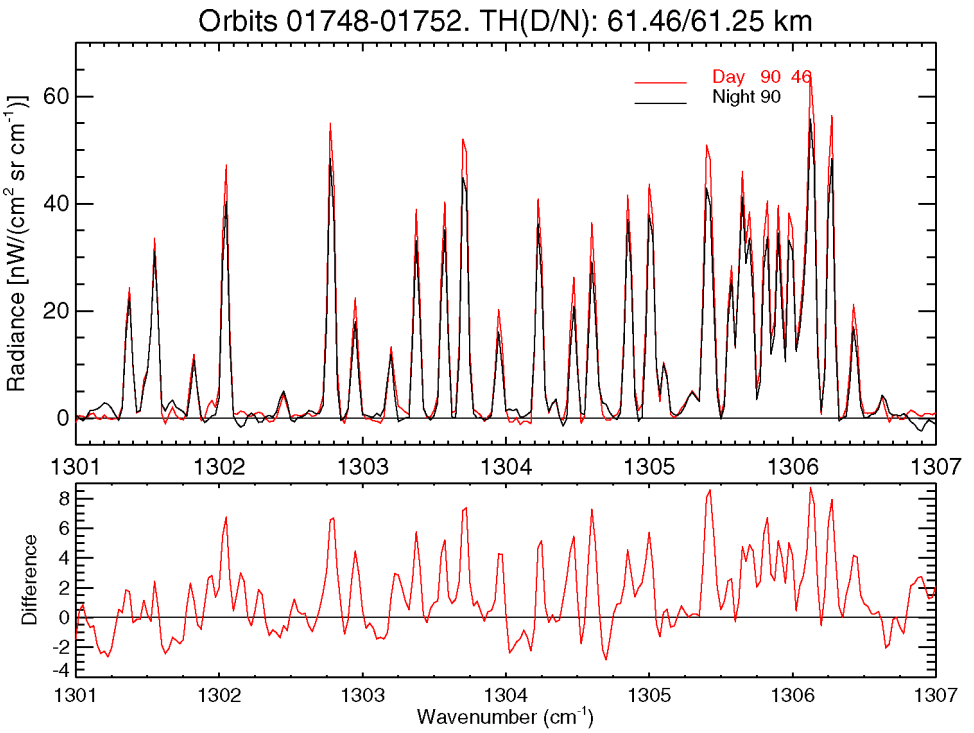

Fig. 8. Day- (broader line/red) and nighttime (fine line/black) averaged MIPAS spectra and their difference for the CH_4 ν_4 fundamental band near 7.6 μm (1300 cm^{-1}). The spectra have been averaged for the 65°S–65°N latitude band for a tangent height of ∼61 km. The effective NESR of the averaged spectra is ∼1.5 nW/(cm^2 sr cm^{-1}). The measurements are from 2 July 2002. (For interpretation of the references to color, the reader is referred to the web version of this article.)

until MIPAS measurements became available. Fig. 8 shows day and nighttime spectra with emission arising from the CH_4 ν_4 level. It clearly shows that the daytime radiance is larger than that at nighttime. Integrating the radiance over all lines of the CH_4 ν_4 fundamental band for the different altitudes and latitudes measured by MIPAS on 2 July 2002, shows that this daytime enhancement occurs at most latitudes and at altitudes above ∼50 km (Fig. 9).

A detailed analysis of this diurnal enhancement has been carried out by López-Puertas et al. [32] and has shown that it can be attributed to a non-LTE enhancement in the population of the ν_4 level. The population of this level is largely controlled by collisions with $O_2(1)$,

$$CH_4 + O_2(1) \leftrightarrow CH_4(v_4) + O_2 \tag{6}$$

Hence, the processes discussed above affecting $O_2(1)$ and $H_2O(010)$, also control the population of $CH_4(\nu_4)$. MIPAS measurements have hence confirmed for the first time the CH_4 ν_4 non-LTE mesospheric emission.

6. NO_2 6.2-μm and NO 5.3-μm stratospheric emissions

The emission from NO_2 in the ν_3 bands around 6.2 μm are commonly used for retrieving the NO_2 atmospheric abundance. Until MIPAS measurements, it had not been clear to which degree the $NO_2(v_3)$ levels, responsible for the emission near 6.2 μm (i.e., 1400–1650 cm^{-1}), are enhanced by non-LTE processes in the daytime stratosphere. Kerridge and Remsberg [33] found evidence for non-LTE emissions at 6.2 μm from measurements taken by the Limb Infrared Monitor of the Stratosphere (LIMS) instrument on board the Nimbus 7 satellite. The chemiluminescence reaction

$$NO + O_3 \rightarrow NO_2(^2B_2/^2A_1, v) + O_2 \tag{7}$$

and the absorption of solar radiation at 400–800 nm

$$NO_2 + h\nu \text{ (400–800 nm)} \rightarrow NO_2(^2B_2/^2A_1, v) \tag{8}$$

followed by radiative and collisional relaxation of $NO_2(^2B_2/^2A_1, v)$:

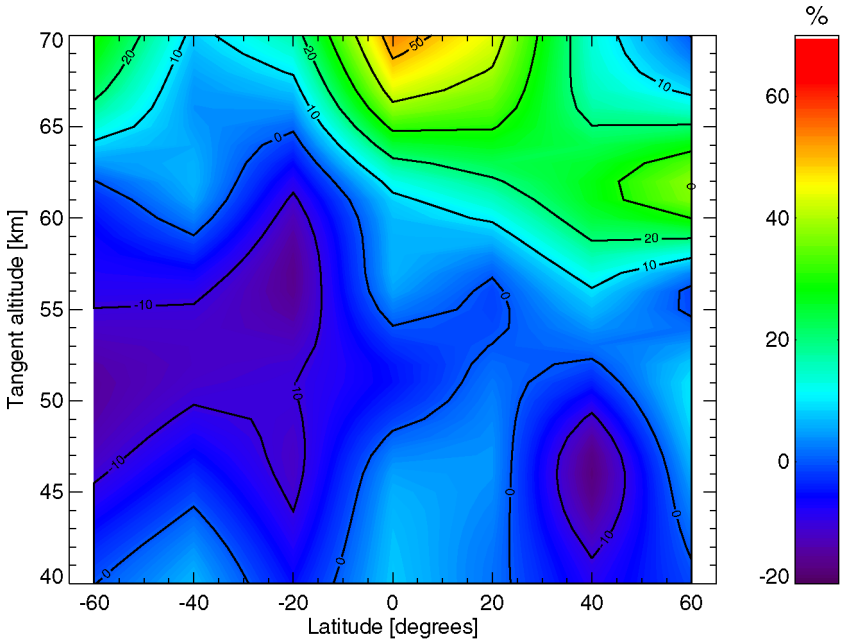

Fig. 9. Zonal mean day–night radiance differences as a function of latitude and tangent altitude in the CH_4 ν_4 fundamental band centred around 7.6 μm in % of nighttime values. The measurements are from 2 July 2002.

$$NO_2(^2B_2/^2A_1, v) \rightarrow NO_2(v_3 \leqslant 7) + h\nu \ (\lambda > 400 \text{ nm}) \tag{9}$$

$$NO_2(^2B_2/^2A_1, v) + M \rightarrow NO_2(v_3 \leqslant 7) + M \tag{10}$$

are thought to be the major sources of non-LTE excitation of the $NO_2(v_3 = 1\text{–}7)$ levels.

Evans and Shepherd [34] reported the existence of a stratospheric airglow layer in the visible (500–1000 nm) and proposed that it originates from electronically excited NO_2 created from the reaction of NO and O_3 (processes (7) and (9)). This finding proves, at least, the existence of an excitation source of $NO_2(^2B_2/^2A_1, v)$. However, whether it is strong enough to excite $NO_2(v_3 = 1\text{–}7)$, or if it is quenched before its energy is transferred to the $NO_2(v_3)$ levels, was not clear.

The analysis of the 6.2-μm emission measured by the Improved Stratospheric and Mesospheric Sounder (ISAMS) showed that the non-LTE excitation of $NO_2(v_3 = 1\text{–}7)$ should be much smaller than those found from the analysis of LIMS measurements [23]. In the same sense, Remsberg et al. [35] have recently re-analysed LIMS radiances (V6) and found that the day/night difference in NO_2 (non-LTE enhancement) is no longer present (E. E. Remsberg, pers. comm., 2004).

The high spectral resolution of MIPAS and its wide spectral coverage have allowed the examination in detail of these non-LTE effects. Funke et al. [36] have recently carried out a very detailed analysis of MIPAS spectra in this region. Including the non-LTE processes discussed above, they have retrieved, simultaneously, the NO_2 abundance from the ν_3 fundamental band, and the photo-chemical excitation rate of $NO_2(v_3 = 1\text{–}7)$ (processes 7 to 10) from the emission in the first hot band ($002 \rightarrow 001$). They then compared the retrieved photo-chemical rate for daytime with that expected from non-LTE models, including the abundances of the required species retrieved from MIPAS, NO, NO_2 and O_3, and using the Tropospheric Ultraviolet-Visible (TUV) radiation model [37]. The values for the collisional quenching rates of $NO_2(v_3)$ in the retrieval and in the model simulation were the same. They found (see Fig. 10) a good correlation between the retrieved and expected rates, hence proving that the proposed mechanisms described above are operating in the excitation of $NO_2(v_3)$. A further evidence of this is that the value retrieved at nighttime is negligible within the measurement errors. However, the value they retrieved for the photo-chemical rate at daytime, 0.42×10^6 cm^3 s^{-1}, is about 50 times smaller than that predicted by the model. Thus, MIPAS has revealed that stratospheric daytime excitation of the $NO_2(v_3 \leqslant 7)$ levels is much smaller than previously thought (e.g., [2,38]).

Apart from the photo-chemical excitation, radiative processes may also generate non-LTE populations of the $NO_2(001)$ level in the upper stratosphere and mesosphere in the polar winter region [2]. This non-LTE deviation significantly depends on the collisional rates of $NO_2(001)$ with N_2 and O_2. These rates are still rather uncertain (∼50%) [38], (B. Toselli, priv. comm., 2005) which still poses an uncertainty of ∼10% in the population of $NO_2(001)$ in the polar winter upper stratosphere.

The non-thermal excitation of NO(1) in the daytime stratosphere was proposed by Kaye and Kumer [39]. They suggested that daytime $NO(v)$ is excited by the following excitation mechanisms:

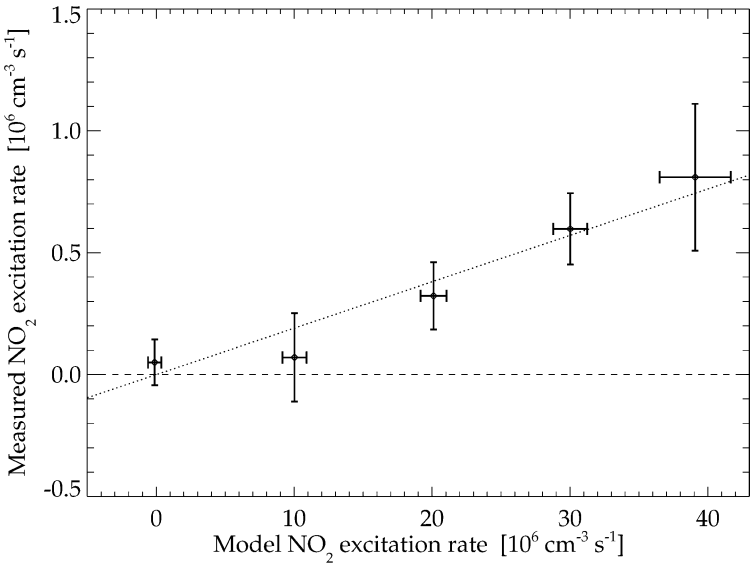

Fig. 10. Measured $NO_2(v_3)$ photo-chemical excitation rates versus modeled. Vertical error bars refer to retrieval errors of the measurement mean values, horizontal error bars represent uncertainties of the model mean values due to retrieval errors of NO_2, O_3, and NO. A regression fit with a slope of 0.02 is shown by a dotted line.

$$NO_2 + O \rightarrow NO(v) + O_2 \tag{11}$$

$$NO_2 + h\nu \rightarrow NO(v) + O \tag{12}$$

These excitation mechanisms have been incorporated into non-LTE models, e.g., [40], but had not been confirmed experimentally until the recent MIPAS measurements. Funke et al. [36] have shown that if these excitation mechanisms are not included in the retrieval of the NO abundance from the 5.3-μm emission, the retrieved stratospheric NO abundance would be significantly overestimated, in contradiction with the expected model results from the photochemical equilibrium between NO and NO_2 during daytime (see Fig. 11). Thus, once more, MIPAS spectra have contributed to improve our knowledge of non-LTE atmospheric processes.

7. Thermospheric NO 5.3-μm emission

The emission from NO at 5.3 μm constitutes the major infrared cooling of the thermosphere and hence its knowledge is very important for computing the energy balance of this atmospheric region. In addition, the abundance of NO and the NO(v) excitation temperatures in this region are so large that they largely contribute to the stratospheric limb paths and hence have to be taken into account when retrieving the stratospheric NO abundances. It is well known that the thermospheric NO(v) emission is in non-LTE but still exist large uncertainties in some parameters, as, for example, the spin and rotational distributions (e.g., [2,40]).

MIPAS has provided spectra of the thermosphere in the 5.3-μm region with the best spectral resolution so far measured. Fig. 12 shows a co-added spectra at a tangent height of ∼101 km, covering part of the NO($1 \rightarrow 0$) band, where it can be appreciated the quality of the measurements. The rotational, as well as the orbit-spin lines are clearly resolved by MIPAS. Furthermore, MIPAS is sensitive enough to measured also the stronger lines of the NO($2 \rightarrow 1$) first hot band (Fig. 13). From these measurements we expect to derive the rotational and spin distribution of the fundamental band, and the vibrational population of the NO(2) level. A preliminary analysis has shown that the spin temperatures are in good agreement with previous measurements and model predictions as in [40]. A detailed analysis of this spectral region, however, has not been performed yet.

8. CO 4.7-μm emissions

MIPAS has also measured the CO emission in the 4.7-μm region. The high spectral resolution allows one to isolate the CO lines from other atmospheric emitters in this region as CO_2, O_3 and N_2O. Fig. 14 shows co-added spectra for day and nighttime conditions at a tangent height of ∼71 km. We clearly distinguish the strong CO lines in the fundamental $1 \rightarrow 0$ band, which are greatly pumped in the daytime due to absorption of solar radiation by CO at 4.7 μm. Non-LTE in this band is reasonably well

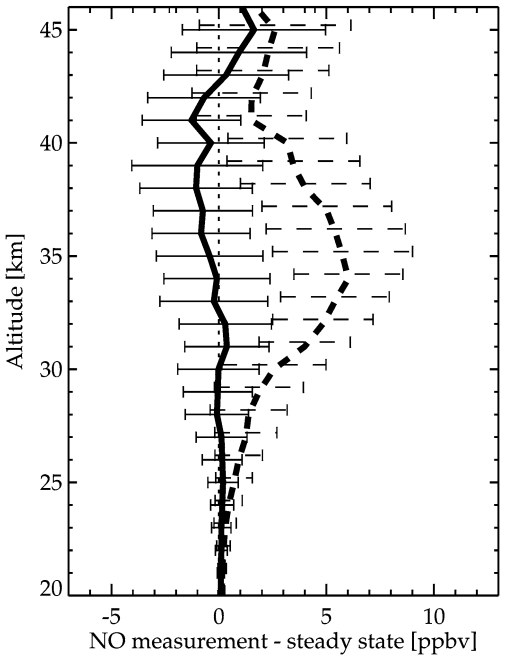

Fig. 11. Differences between measured daytime NO and calculated daytime NO assuming photochemical equilibrium between NO and NO_2. Mean values and 1-σ variances (bars) of the differences are shown versus altitude. The differences are shown for the retrieved NO including (solid) and excluding (dashed) non-LTE excitation processes (11) and (12) for NO(v).

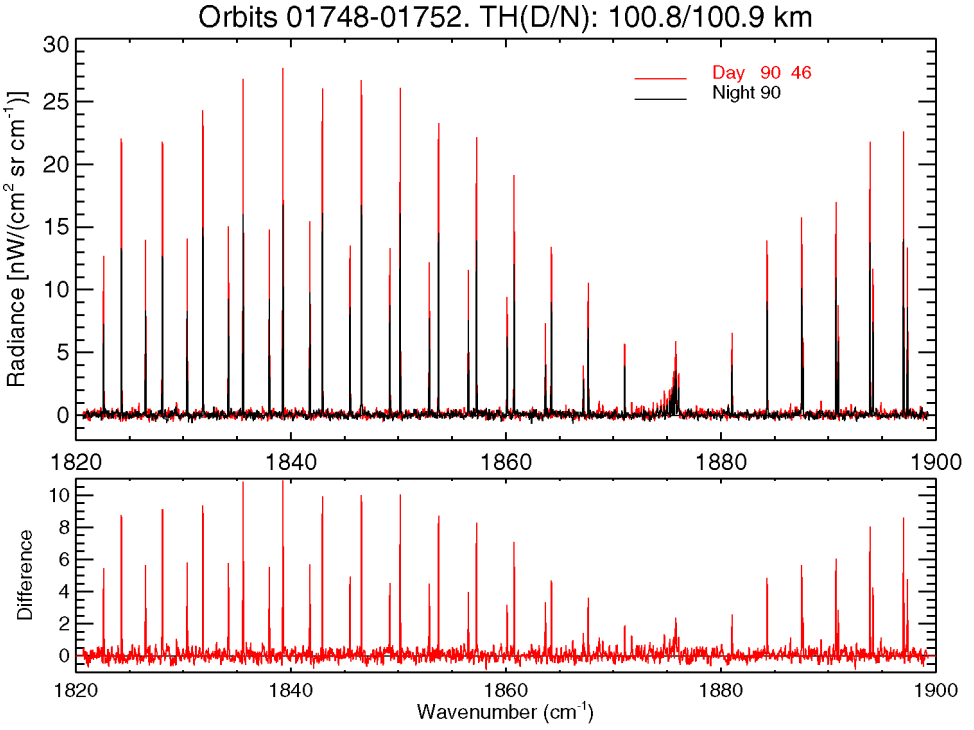

Fig. 12. Day- (dotted/red) and nighttime (solid/black) co-added MIPAS spectra and their difference in the region of the NO 5.3-μm emission. The spectra have been co-added for the 65°S–65°N latitude band for a tangent height of ∼101 km. The effective NESR of the co-added spectra is ∼0.3 nW/(cm^2 sr cm^{-1}). The measurements are from 2 July 2002. (For interpretation of the references to color, the reader is referred to the web version of this article.)

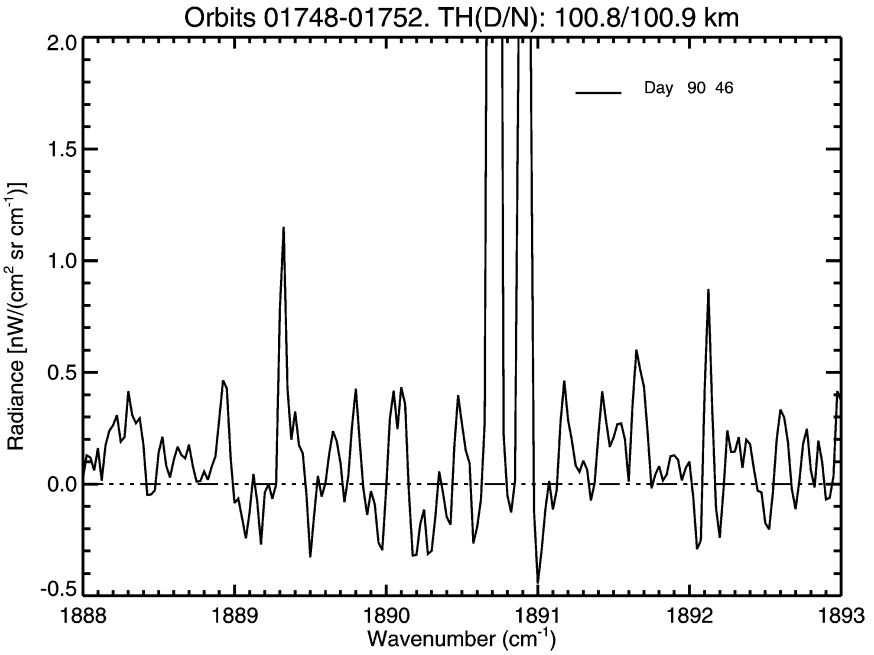

Fig. 13. A zoom of Fig. 12 showing contribution lines of the NO($2 \rightarrow 1$) band near 1889.3 and 1892.15 cm^{-1}.

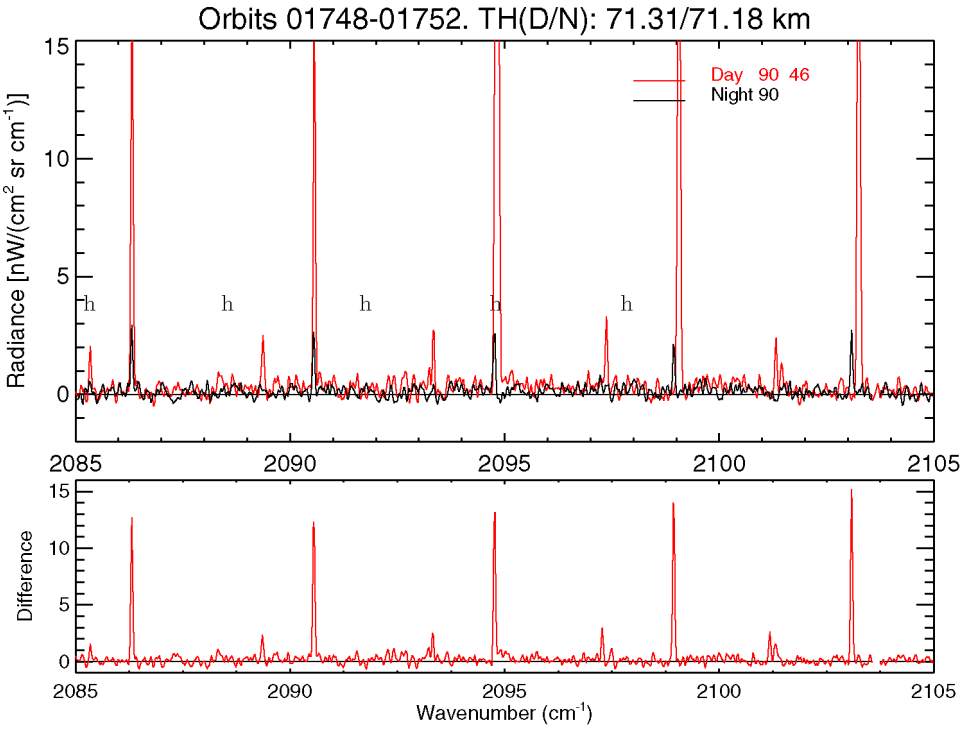

Fig. 14. MIPAS spectra in the 4.7 μm region dominated by the CO fundamental ($1 \rightarrow 0$) band (stronger lines). CO first hot ($2 \rightarrow 1$) transitions (h) are also observed. Upper panel: day (dotted/red), mean SZA = 46°, and nighttime (solid/black) spectra. 90 spectra were co-added for each case of day and nighttime. Lower panel: day–night difference spectra. The spectra were measured on 2nd July 2002 and cover latitudes from 65°S to 65°N. (For interpretation of the references to color, the reader is referred to the web version of this article.)

known [2] and it is being used for retrieving the CO abundance [41,42]. In addition to this, the weak emission lines arising near 2085.2, 2089.3, 2093.4, 2097.3 and 2101.3 cm^{-1} in the spectra are also noticeable, which coincide with the line positions of the CO $2 \rightarrow 1$ first hot band. This is the first time that these emissions have been detected in the atmosphere. A preliminary analysis has shown that they are reasonably simulated by the absorption of solar radiation by CO in the $2 \rightarrow 0$ band near 2.3 μm. Note that its emission at nighttime is completely negligible. A detailed analysis of this emission is in progress.

9. Summary and conclusions

In this article we report the most recent advances in our knowledge of non-LTE atmospheric emissions gained from the spectra measured by MIPAS on the Envisat satellite. MIPAS has several advantages which makes it an excellent instrument for studying the atmospheric non-LTE emissions. In particular:

(i) its wide spectral coverage (4.15–14.6 μm or 680–2275 cm^{-1}) allows for measuring emissions from a given compound in different spectral regions;
(ii) its high spectral resolution (0.035 cm^{-1}) enables to discriminate emissions from different species and from different bands of the same species; and
(iii) its high sensitivity allows us to measure the faint emission from the upper atmosphere where non-LTE emissions are most important.

We report here improvements in non-LTE parameters related to the species CO_2, O_3, H_2O, CH_4, NO_2, NO and CO.

New collisional rates between the CO_2 02^00, 02^20, and 10^01 states, emitting the 4.3-μm second hot bands, have been derived and differ largely, by factors of 3.5 and 0.025, from previously consensus values.

Concerning non-LTE in O_3, a preliminary analysis of MIPAS spectra in the 2080–2130 cm^{-1} region has shown that a typical non-LTE model, underestimates the MIPAS daytime radiance by a factor of 2–3 in the 60–70 km region. Possible reasons for explaining this discrepancy are that O_3 is formed at lower vibrational levels, and/or the collisional relaxation of the stretching (v_1, v_3) is weaker [20].

MIPAS has taken the most unequivocal spectra so far obtained demonstrating clearly the distinct non-LTE daytime emissions from the fundamental and hot bands of H_2O 6.3-μm bands for each altitude and latitude separately with an excellent signal-to-noise ratio. The most accurate collisional rate for the relaxation of $H_2O(020)$ by O_2 has been obtained, with a value of 1.36×10^{-12} $cm^3\,s^{-1}$ with a 10% uncertainty [26] and the rate of quenching of $O_2(1)$ by atomic oxygen $O(^3P)$ measured by Pejaković et al. [27] has been further confirmed [26].

MIPAS spectra have for the first time revealed the non-LTE mesospheric emission of the daytime CH_4 ν_4 emission [32].

MIPAS has also made possible to throw light on the puzzle about whether or not the $NO_2(v_3)$ levels are non-LTE excited in the daytime stratosphere. A recently analysis has shown [36] that the photochemical excitation of $NO_2(v_3 = 1\text{–}4)$ levels is a factor of 50 smaller than previously thought, leading to small non-LTE deviations for these levels.

In addition, MIPAS has given the first experimental confirmation of the non-LTE processes exciting NO(1) (5.3-μm emission) in the daytime stratosphere [36] as proposed by [39]. MIPAS have also resolved the NO rotational and spin transitions in the 5.3-μm emission in the thermosphere. A preliminary analysis have confirmed previous spin temperatures.

Finally, it has also shown the first measurement in the atmosphere of the CO first hot band emission near 4.7 μm in the daytime atmosphere.

Although the amount of knowledge on non-LTE atmospheric processes already gained is enormous, the full exploitation of MIPAS spectra still remains to be done. Most of the studies described here are still rather preliminary and incomplete, and emissions from other species will also be studied.

Acknowledgement

The IAA team has been supported by Spanish Ministerio de Educación y Ciencia under projects REN2001-3249/CLI and ESP2004-01556, EC FEDER funds, and by the European Community Marie Curie Host Fellowship HPMD-CT-2000-40 (SIESTA). IMK was partially supported by German projects SACADA (07ATF53) and KODYACS (07ATF43).

References

[1] F.W. Taylor, M. López-Puertas, Radiative transfer: Non local thermodynamic equilibrium, in: J.R. Holton, J. Pyle, J.A. Curry (Eds.), Encyclopedia of Atmospheric Sciences, Academic Press, Amsterdam, 2003, pp. 1874–1882.

[2] M. López-Puertas, F.W. Taylor, Non-LTE Radiative Transfer in the Atmosphere, World Scientific Publishing Co., Singapore, 2001.
[3] P.P. Wintersteiner, R.H. Picard, R.D. Sharma, J.R. Winick, R.A. Joseph, Line-by-line radiative excitation model for the non-equilibrium atmosphere: application to CO_2 15 μm emission, J. Geophys. Res. 97 (1992) 18083–18117.
[4] H. Nebel, P.P. Wintersteiner, R.H. Picard, J.R. Winick, R.D. Sharma, CO_2 non-local thermodynamic equilibrium radiative excitation and infrared dayglow at 4.3 μm: Application to spectral infrared rocket experiment data, J. Geophys. Res. 99 (1994) 10409–10419.
[5] G.M. Shved, A.A. Kutepov, V.P. Ogibalov, Non-local thermodynamic equilibrium in CO_2 in the middle atmosphere I. Input data and populations of the ν_3 mode manifold states, J. Atmos. Solar-Terr. Phys. (1997) 2167–2176.
[6] H. Fischer, H. Oelhaf, Remote sensing of vertical profiles of atmospheric trace constituents with MIPAS limb-emission spectrometers, Appl. Opt. 35 (16) (1996) 2787–2796.
[7] European Space Agency, Envisat, MIPAS An instrument for atmospheric chemistry and climate research, ESA Publications Division, ESTEC, The Netherlands, SP-1229, 2000.
[8] K.U. Grossmann, D. Offermann, O. Gusev, J. Oberheide, M. Riese, R. Spang, The CRISTA-2 mission, J. Geophys. Res. 107 (D23) (2002) 8173, doi:10.1029/2001JD000667.
[9] J.M. Russell III, M.G. Mlynczak, L.L. Gordley, J. Tansock, R. Esplin, An overview of the SABER experiment and preliminary calibration results, in: Proc. SPIE, vol. 3756, 1999, pp. 277–288.
[10] M. López-Puertas, F.W. Taylor, Carbon dioxide 4.3-μm emission in the Earth's atmosphere. A comparison between NIMBUS 7 SAMS measurements and non-LTE radiative transfer calculations, J. Geophys. Res. 94 (1989) 13045–13068.
[11] M. López-Puertas, M.G. Zaragoza, M.A. López-Valverde, F.W. Taylor, Non local thermodynamic equilibrium (LTE) atmospheric limb emission at 4.6 μm I. An update of the CO_2 non-LTE radiative transfer model, J. Geophys. Res. 103 (1998) 8499–8513.
[12] M. López-Puertas, M.G. Zaragoza, M.A. López-Valverde, F.W. Taylor, Non-LTE atmospheric limb radiances at 4.6 μm as measured by UARS/ISAMS II. Analysis of the daytime radiances, J. Geophys. Res. 103 (1998) 8515–8530.
[13] M. Kaufmann, O.A. Gusev, K.U. Grossmann, R.G. Roble, M.E. Hagan, C. Hartsough, A.A. Kutepov, The vertical and horizontal distribution of CO_2 densities in the upper mesosphere and lower thermosphere as measured by CRISTA, J. Geophys. Res. 107 (D23) (2002) 8182, doi:10.1029/2001JD000704.
[14] C.J. Mertens, M.G. Mlynczak, M. López-Puertas, P.P. Wintersteiner, R.H. Picard, J.R. Winick, L.L. Gordley, J.M. Russell III, Retrieval of kinetic temperature and carbon dioxide abundance from non-local thermodynamic equilibrium limb emission measurements made by the SABER experiment on the TIMED satellite, in: Proc. SPIE, vol. 4882, 2002, pp. 162–171.
[15] G.P. Stiller, T. von Clarmann, B. Funke, N. Glatthor, F. Hase, M. Höpfner, A. Linden, Sensitivity of trace gas abundances retrievals from infrared limb emission spectra to simplifying approximations in radiative transfer modelling, J.Q.S.R.T 72 (3) (2002) 249–280.
[16] B. Funke, F.J. Martín-Torres, M. López-Puertas, M. Höpfner, F. Hase, M.Á. López-Valverde, M. García-Comas, A generic non-LTE population model for MIPAS–ENVISAT data analysis, Geophys. Res. Abs. 4 (2002).
[17] M. López-Puertas, et al., Mesospheric and lower thermospheric temperature and carbon dioxide volume mixing ratio as measured by MIPAS/Envisat, Geophys. Res. Abs. 6 (2004) 04672.
[18] S. Gil-López, M. Kaufmann, B. Funke, M. García-Comas, M.E. Koukouli, M. López-Puertas, N. Glatthor, U. Grabowski, M. Höpfner, G.P. Stiller, T. von Clarmann, Retrieval of stratospheric and mesospheric O_3 from high resolution MIPAS spectra at 15 and 10 μm, Adv. Spa. Res. (2005), in press.
[19] M. Kaufmann, O.A. Guzev, K.U. Grossmann, F.J. Martín-Torres, D.R. Marsh, A.A. Kutepov, Satellite observations of daytime and nighttime ozone in the mesosphere and lower thermosphere, J. Geophys. Res. 108 (D9) (2003) 4272, doi:10.1029/2002JD002800.
[20] M. Kaufmann, S. Gil-López, M. López-Puertas, B. Funke, M. García-Comas, M.E. Koukouli, N. Glatthor, U. Grabowski, M. Höpfner, G.P. Stiller, T. von Clarmann, L. Hoffmann, M. Riese, Vibrationally excited ozone in the middle atmosphere, J. Atmos. Solar Terr. Phys., 2005, submitted for publication.
[21] J. Menard, L. Doyennette, F. Menard-Bourcin, Vibrational relaxation of ozone in O_3–O_2 and O_3–N_2 gas mixtures from infrared double-resonance measurements in the 200–300 K temperature range, J. Chem. Phys. 96 (1992) 5773.
[22] F. Menard-Bourcin, L. Doyennette, J. Menard, Vibrational energy transfer in ozone excited into the (101) state from double-resonance measurements, J. Chem. Phys. 101 (1994) 8636.
[23] G. Zaragoza, M. López-Puertas, A. Lambert, J.J. Remedios, F.W. Taylor, Non-local thermodynamic equilibrium in H_2O 6.9 μm emission as measured by the Improved Stratospheric and Mesospheric Sounder, J. Geophys. Res. 103 (1998) 31293–31308.
[24] D.K. Zhou, M.G. Mlynczak, M. López-Puertas, G. Zaragoza, Evidence of non-LTE effects in mesospheric water vapour from spectrally-resolved emissions observed by CIRRIS-1A, Geophys. Res. Lett. 26 (1999) 67–70.
[25] D.P. Edwards, G. Zaragoza, M. Riese, M. López-Puertas, Evidence of H_2O non-local thermodynamic equilibrium emission near 6.4 μm as measured by CRISTA-1, J. Geophys. Res. 105 (2000) 29003–29022.
[26] M.E. Koukouli, M. López-Puertas, B. Funke, S. Gil-López, M. Kaufmann, M. Milz, T. von Clarmann, G.P. Stiller, Water vapour 6.3 μm non-local thermodynamic equilibrium emissions as measured by MIPAS/Envisat, J. Geophys. Res. (2005), submitted for publication.
[27] D.A. Pejaković, Z. Campbell, K.S. Kalogerakis, R.A. Copeland, T.G. Slanger, Rate coefficient for collisional removal of $O_2(X^3\Sigma_g^-, v = 1)$ with O atoms at 240 K, Eos Trans. AGU 85 (47) (2004), Fall Meet. Suppl., Abstract SA41A-1032.
[28] R.L. Jones, J.A. Pyle, Observations of CH_4 and N_2O by the NIMBUS 7 SAMS: A comparison with in situ data and two dimensional numerical model calculations, J. Geophys. Res. 89 (D4) (1984) 5263–5279.
[29] J.J. Remedios, et al., Measurements of methane and nitrous oxide distributions by the improved stratospheric and mesospheric sounder: Retrieval and validation, J. Geophys. Res. 101 (1996) 9843–9871.
[30] G.M. Shved, O.A. Gusev, Non-local thermodynamic equilibrium in N_2O, CH_4, and HNO_3 in the middle atmosphere, J. Atmos. Solar-Terr. Phys. 59 (1997) 2167–2176.

[31] F.J. Martín-Torres, M.A. López-Valverde, M. López-Puertas, Non-LTE populations of CH_4 and N_2O for MIPAS/Envisat-1, J. Atmos. Solar-Terr. Phys. 60 (1998) 1631–1647.
[32] M. López-Puertas, M.E. Koukouli, B. Funke, S. Gil-López, N. Glatthor, U. Grabowski, T. von Clarmann, G.P. Stiller, Evidence for CH_4 7.6 μm non-local thermodynamic equilibrium emission in the mesosphere, Geophys. Res. Lett. 32 (2005) L04805, doi:10.1029/2004GL021641.
[33] B.J. Kerridge, E.E. Remsberg, Evidence from the limb infrared monitor of the stratosphere for nonlocal thermodynamic equilibrium in the ν_2 mode of mesospheric water vapour and the ν_3 mode of stratospheric nitrogen dioxide, J. Geophys. Res. 94 (D13) (1989) 16323–16342.
[34] W. Evans, G. Shepherd, A new airglow layer in the stratosphere, Geophys. Res. Lett. 23 (24) (1996) 3623–3626.
[35] E. Remsberg, L. Gordley, B. Marshall, R. Thompson, P.B.J. Burton, V. Harvey, G. Lingenfelser, M. Natarajana, The Nimbus 7 LIMS version 6 radiance conditioning and temperature retrieval methods and results, J. Quant. Spectrosc. Radiat. Transfer 86 (2004) 395–424.
[36] B. Funke, M. López-Puertas, T. von Clarmann, G.P. Stiller, H. Fischer, N. Glatthor, U. Grabowski, M. Höpfner, S. Kellmann, M. Kiefer, A. Linden, G. Mengistu-Tsidu, M. Milz, T. Steck, D.Y. Wang, Retrieval of stratospheric NO_x from 5.3 and 6.2 μm non-LTE emissions measured by MIPAS on ENVISAT, J. Geophys. Res. 110 (2005) D09302, doi:10.1029/2004JD005225.
[37] S. Madronich, S. Flocke, The role of solar radiation in atmospheric chemistry, in: P. Boule (Ed.), Handbook of Environmental Chemistry, Springer-Verlag, Heidelberg, 1998, pp. 1–26.
[38] M. López-Puertas, Assessment of NO_2 non-LTE effects in MIPAS spectra, Tech. Rep., European Space Agency, 1997. Final Report of ESA Contract 12054/96/NL/CN.
[39] J.A. Kaye, J.B. Kumer, Nonlocal thermodynamic equilibrium effects in stratospheric NO and implications for infrared remote sensing, Appl. Opt. 26 (22) (1987) 4747–4754.
[40] B. Funke, M. López-Puertas, Nonlocal thermodynamic equilibrium vibrational, rotational, and spin state distribution of NO($\nu = 0, 1, 2$) under quiescent atmospheric conditions, J. Geophys. Res. 105 (D4) (2000) 4409–4426.
[41] B. Funke, et al., CO in the middle atmosphere measured with MIPAS/ENVISAT, Geophys. Res. Abstracts, 6, 04358, SRef-ID: 1607-7962/gra/EGU04-A-04358, 2004.
[42] B. Funke, et al., Carbon monoxide observations by MIPAS/Envisat during the major warming event in September/October 2002, J. Geophys. Res. (2005), submitted for publication.